REFERENCES

1. Unwin, P. N. T., and R. Henderson. 1975. Molecular structure determination by electron microscopy of unstained crystalline specimens. *J. Mol. Biol.* 94:425–440.
2. Vainshtein, B. K. 1978. Electron microscopical analysis of the three-dimensional structure of biological macromolecules. *Adv. Opt. Electron Microsc.* 7:281–377.
3. Steven, A. C., and M. A. Navia. 1982. Specificity of stain distribution in electron micrographs of protein molecules contrasted with uranyl acetate. *J. Microsc.* 128:145–155.
4. Erickson, H. P. 1973. The Fourier transform of an electron micrograph-first order and second order theory of image formation. *Adv. Opt. Electron Microsc.* 5:163–199.
5. Engel, A., and A. Massalski. 1984. 3D reconstruction from electron micrographs: Its potential and practical limitations. *Ultramicroscopy.* 13:71–84.
6. Dorset, D. L., 1984. Dynamical electron scattering from negatively stained protein microcrystals. *Ultramicroscopy.* 13:311–324.
7. Klug, A. 1978-1979. Image analysis and reconstruction in the electron microscopy of biological macromolecules. *Chem. Scripta.* 14:245–256.
8. Dorset, D. L., A. Engel, A. Massalski, and J. P. Rosenbusch. 1984. Three-dimensional structure of a membrane pore. Electron microscopical analysis of *Escherichia coli* outer membrane matrix porin. *Biophys. J.* 45:128–129.
9. Grinton, G. R., and J. M. Cowley. 1971. Phase and amplitude contrast in electron micrographs of biological material. *Optik.* 34:221–233.
10. Baldwin, J., and R. Henderson. 1984. Measurement and evaluation of electron diffraction patterns from two-dimensional crystals. *Ultramicroscopy.* 14:319–336.
11. Cowley, J. M. 1961. Diffraction intensities from bent crystals. *Acta Crystallogr.* 14:920–927.
12. Dorset, D. L. 1983. Electron crystallography of alkyl chain lipids; identification of long chain packing. *Ultramicroscopy.* 12:19–28.
13. Dumont, M. E., J. W. Wiggins, and S. B. Hayward. 1980. Electron diffraction of platinum labeled bacteriorhodopsin. Proc. Electron Microsc. Soc. America, 38th Annual Meeting, San Francisco, CA. Claitor's Press, Baton Rouge. 34–35.
14. Doyle, P. A., and P. S. Turner. 1968. Relativistic Hartree-Fock x-ray and electron scattering factors. *Acta Crystallogr.* A24:390–397.

HYDRATED MACROMOLECULAR ASSEMBLY STRUCTURE REVEALED BY FREEZE-ETCH STEREO-ELECTRON MICROSCOPY

Spermidine-DNA Toruses and RNA Polymerase-DNA Complexes

KENNETH A. MARX AND GEORGE C. RUBEN

Departments of Chemistry and Biology, Dartmouth College, Hanover, New Hampshire 03755

Hydrated macromolecules can be visualized using the freeze-fracture, deep-etch (FET) protocol. By fracturing, etching the specimen at -100°C, then cooling it to -174°C in a 5×10^{-8} torr vacuum, a 7–10 Å surface coating of Pt-C (45°) can resolve 10–20 Å specimen surface details by using transmission electron microscopy (TEM). In contrast to uncoated molecules, which begin disintegrating during the first micrograph, 10 or more micrographs in a tilt series of a single Pt-C coated molecule can be recorded with a eucentric goniometer without specimen replica deterioration. Using pairs of stereomicrographs of magnification M, separated by the tilt angle θ, parallax measurements of height H can reveal three-dimensionsal topography of macromolecular complexes using the parallax equation

$$H = (P_H - P_L)/2M \sin(\theta/2). \quad (1)$$

This methodology has advantages over other preparative and physical techniques. The FET visualizes hydrated specimens, whereas other EM techniques require a dehydrated specimen or embedding in the high salt and unusual pH of negative stains. Unlike x-ray or neutron diffraction and NMR spectroscopy, which look at ordered or freely diffusing molecular populations in large mass quantities, in FET individual molecules are imaged in submicrogram quantities in a noncrystalline sample. Furthermore, the FET may be applied to any kind of macromolecular assembly, and stereoscopic height measurements from the object replica have been shown to achieve a 95% fractile precision in the 5–10 Å range (1). Stereoscopic imaging complements structural data obtained by x-ray and neutron diffraction, light scattering and, to a much lesser extent, NMR spectroscopy. In contrast to light and neutron scattering, FET can measure the dimensions and topographic features of individual objects in a series of tilt views rather than fitting an averaged scattering intensity to a generalized model scattering object. This advantage is illustrated by the two systems presented here: the spermidine-condensed DNA toruses, which are in vitro model systems for DNA packing in bacteriophage and certain viruses, and the RNA polymerase-DNA ternary complex.

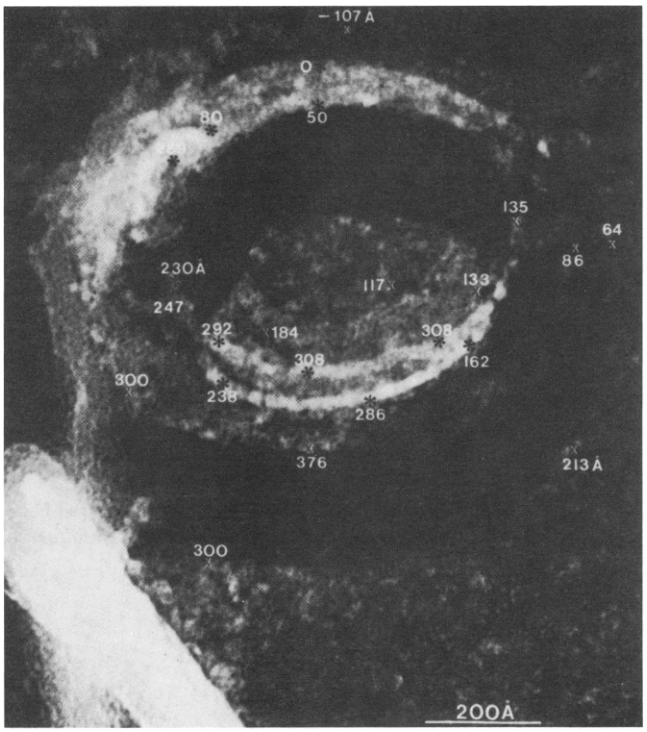

FIGURE 1 Mirror stereoscope height measurements of DNA topology in a spermidine-calf thymus DNA torus. All points, in Å units, were measured using $10^6\times$ prints of two torus tilt views separated by 10°.

RESULTS

In the first system we obtained information on individual torus dimensions within a population. Although time-consuming, it yielded detailed information that light scattering cannot quantitatively yield such as the existence and measured sizes of monomer and distinct multimer DNA torus classes (2). Moreover, we obtained unique additional information represented by Fig. 1: direct visualization of circumferential DNA winding, the major DNA tertiary structure organization in these objects, and measurements of the detailed topology of individual DNA strands to a high precision (10 Å). The unique nature of the torus dimensions measurable by FET TEM from a linear DNA size series (Table I) suggests some simple principles of torus self-assembly. The monomer DNA fragment size results from gel electrophoresis of DNA digested in the condensed state by micrococcal nuclease. We postulate that the monomer fragment results from two cleavage events in the same torus region but on either end of one circumferential DNA length winding about the torus (3, 4). Besides support for the circumferential winding of DNA provided by our direct strand visualizations (Fig. 1), a consequence of this particular model requires that the monomer fragment size be flanked by the measured inner and outer circumference values of the torus populations. This is the case for all three DNA molecules.

Principles concerning the progression of DNA self-assembly may also be drawn uniquely from these data. The ϕX-174 DNA torus parameters support a model of a thin, relatively wide disk-shaped torus (2). This DNA must self-assemble with minimum hexagonal packing by preferentially condensing so as to lower the helix curvature of successive strands (favored energetically). However, in lowering the total free energy, self-assembly will try to maximize helix-helix interactions and minimize energetically unfavorable helix-solution interactions. Therefore, for larger DNA, self-assembly will not only continue in the plane of the torus ring (Fig. 1, page plane) but will proceed progressively to pack hexagonally in the orthogonal (out-of-page) direction, forming a thicker disk with more helix-helix interactions. This is consistent with the CT DNA torus data showing increased disk thickness by stereoscopic measurement (1). Lambda DNA toruses, containing 2.4–8.9-fold as much DNA as the CT and ϕX-174 toruses, have correspondingly larger torus dimensions. Self-assembly of λ DNA strands occurs in both the torus ring plane and orthogonal direction, producing larger, thicker toruses with less DNA curvature (higher average inner circumference) than either ϕX-174 or CT DNA toruses.

The second system we consider is the important cellular protein-nucleic acid interaction of RNA polymerase with DNA. This system has been little studied by physical techniques because of its complexity and the difficulty of obtaining large mass quantities of the complex. Primarily through a very sophisticated neutron scattering approach using label triangulation with selectively deuterated subunits and H_2O/D_2O contrast matching, the intact RNA polymerase holoenzyme has been recently modeled as to general shape and subunit arrangement in the absence of

TABLE I
TORUS PARAMETERS

DNA	MW (bp)	Monomer fragment (bp)	Freeze-etch TEM torus parameters			
			Inner (bp)	Outer (bp)	Ring thickness (Å)	End-on view (Å)
ϕx-174	5386	830 ± 120	539 ± 165	858 ± 75	169 ± 15	30–43
CT	20000	760 ± 87	541 ± 60	825 ± 65	143 ± 18	(60)
λ	48000	1003 ± 115	682 ± 123	1086 ± 120	200 ± 17	60–210

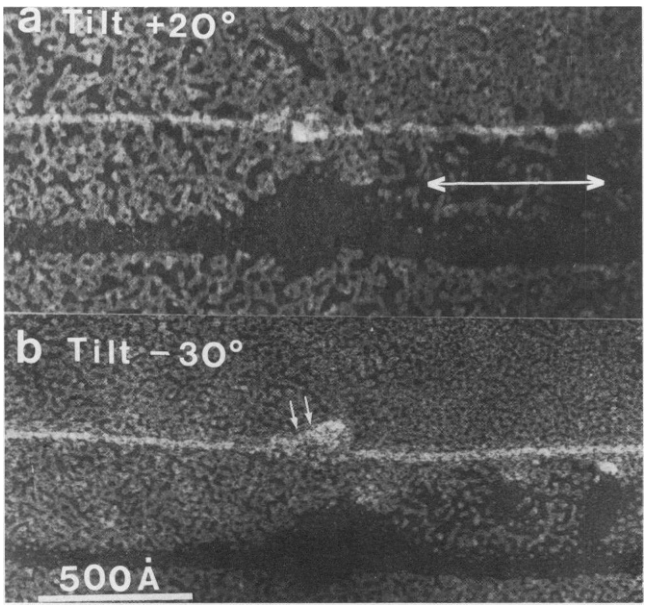

FIGURE 2 Two tilt views of an *E. coli.* RNA polymerase-pBR322 DNA ternary complex. The large arrow indicates the replica tilt axis.

DNA (5). There have been few attempts to visualize the intact RNA polymerase-DNA complex by high-resolution TEM, but we have begun a study of the *Escherichia coli* RNA polymerase-pBR322 DNA ternary complex. Fig. 2 shows two widely separated tilt views of a single RNA polymerase-DNA ternary complex. The tilt view in (*a*), +20°, appears to look down on the wedge-shaped RNA polymerase as its elongated β and β' subunits bind lengthwise along the DNA helix. This interpretation is in general agreement with the wedge-shaped model for polymerase and its binding to DNA proposed by the neutron scattering study (5). In the tilt view in (*b*), −30°, RNA polymerase is being visualized more from the side and the putative position of the σ subunit (neutron study) contacting the β and β' subunits is indicated by small arrows. This complex appears to cover some 60–65 bp of DNA helix, consistent with estimates from enzymatic digestion protection experiments. Furthermore, the DNA helix appears intact at either end of the complex, in general agreement with the estimates of not more than 17 bp DNA unwound in the complex (6).

As these two systems illustrate, any complex hydrated macromolecular assembly can be visualized by FET TEM. Using very low Pt/C metal replicas to preserve surface detail, extensive object tilt series combined with a stereoscopic measurement/surface mapping approach can yield data that is unique or that complements information obtained by other physical techniques.

K. A. Marx acknowledges grants CA23108 from the National Cancer Institute; GM 25886 and Al 17586 from the National Institutes of Health. He also acknowledges grants 8859 from the Research Corp and BRSG 05392 from the Department of Human Health Services. G. C. Ruben acknowledges grant CA 23108 from the National Cancer Institute. K. A. Marx and G. C. Ruben both acknowledge support from Geo M Co. and the generous gift of RNA polymerase-DNA ternary complex from John E. Hearst.

Received for publication 30 April 1985.

REFERENCES

1. Ruben, G. C., and K. A. Marx. 1984. Parallax measurements on stereomicrographs of hydrated single molecules, their accuracy and precision at high magnification. *J. Electron Microsc. Technique.* 1:373–385.
2. Marx, K. A., and G. C. Ruben. 1985. DNA tertiary structure of disk-shaped toruses: an in vitro viral DNA model system. *In* The Molecular Basis of Cancer. 172A. R. Rein, editor. Alan R. Liss, Co., New York. 131–140.
3. Marx, K. A., and T. C. Reynolds. 1982. Spermidine-condensed ϕX-174 DNA cleavage by micrococcal nuclease: torus cleavage model and evidence for unidirectional circumferential DNA wrapping. *Proc. Natl. Acad. Sci. USA.* 79:6484–6488.
4. Marx, K. A. and G. C. Ruben. 1984. Studies of DNA organization in hydrated spermidine-condensed DNA toruses and spermidine-DNA fibres. *J. Biomol. Struct. Dyn.* . 1:1109–1132.
5. Stockel, P., R. May, I. Strell, C. Zdenka, W. Hoppe, H. Heumann, W. Zillig, and H. L. Crespi. 1980. The subunit positions within RNA polymerase holoenzyme determined by triangulation of centre-to centre distances. *Eur. J. Biochem.* 112:419–423.
6. Gamper, H. B., and J. E. Hearst. 1982. A topological model for transcription based on unwinding angle analysis of *E. coli.* RNA polymerase binary, initiation and ternary complexes. *Cell.* 29:81–90.